Research paper

Fragment velocity measurement of steel container during explosion tests by using high-speed and flash X-ray photography

Kunihiko Wakabayashi†, Tomotaka Homae, Koki Ishikawa, Eishi Kuroda, Tomoharu Matsumura, and Yoshio Nakayama

Research Core for Explosion Safety,
Research Institute of Science for Safety and Sustainability,
National Institute of Advanced Industrial Science and Technology (AIST),
Tsukuba Central 5, Higashi 1-1-1, Tsukuba, Ibaraki 305-8565, JAPAN
Tel : +81-29-861-4792, Fax : +81-29-861-4783
†Corresponding address : k-wakabayashi@aist.go.jp

Received : September 25, 2008 Accepted : April 14, 2009

Abstract

Explosion tests were performed using a steel container filled with explosive to determine fundamental properties such as flight velocity, direction, and distribution of fragments. A cylindrical steel container filled with trinitrotoluene (TNT) was prepared as a test sample representing a one-ton bomb. The length to inner diameter ratio (L/I.D.) of the container was set to about two. Images of flying fragments were recorded by a high-speed camera in field explosion tests, and by two flash X-ray tubes and film in indoor explosion tests. In the case where the direction from the center of the container to its open end was defined to be an azimuthal angle of zero degrees, many fragments were distributed at azimuthal angles of around 100 degrees. In an explosion using a container with 1 kg of TNT, the highest fragment velocity determined by the time-of-flight method was 1700 ± 50 $m \cdot s^{-1}$ at a distance of 11.56 ± 0.01 m from the explosion point. However, the initial fragment velocity determined by flash X-ray photography was 2194 $m \cdot s^{-1}$. Thus, the fragment velocities determined by different photographic techniques did not agree. This discrepancy between the observed fragment velocities could be explained by assuming that the fragment velocity depends solely on air resistance.

Keywords : steel container, fragment velocity, high-speed photography, flash X-ray photography, air resistance

1. Introduction

In accordance with a 1996 protocol relating to the International Convention on the Prevention of Marine Pollution by Dumping of Wastes and Other Matter 1972 (London Convention), the disposal of waste in the ocean has been prohibited in Japan since April 2007[1]. Explosives that had formerly been disposed of in the ocean, such as unexploded bombs, were henceforth disposed of on land. This necessitated establishing a technical criterion for the safe handling and disposal of unexploded bombs and ammunitions above ground.

The detonation of a container filled with explosives involves the risk of serious damage to the surroundings as a result of factors such as the blast wave[2-4] and fragments[5-7]. With certain exceptions (e.g., explosions in magazines and structures), the effects of a blast and the induced radiation are considered to decrease gradually with distance from the epicenter of the explosion. However, the effects of fragments depend not only on distance, but also on many other factors, including velocity, flight angle, shape, size, and number. Therefore, it is difficult to accurately estimate the effects of fragments, and these effects could extend over several hundred meters under certain conditions.

Explosion tests using a steel container filled with explosive were carried out to obtain fundamental information needed to evaluate the influence of fragments generated by the explosion of bombs and ammunition. The purpose

Table 1 Specifications of steel containers filled with explosive.

Experiment number	Test site	Container size (mm)							Container mass (kg)	TNT mass(kg)	Booster mass (kg)	Height of burst*** (m)
		L	l	O.D.	I.D.	t1	t2	t3				
2-3	field	143.0	24.1	78.0	72.6	2.7	5.0	6.0	0.97	0.98	0.1*	0.18
2-1-3	field	226.0	38.8	123.9	115.0	4.5	8.0	10.0	3.99	3.96	0.2*	0.29
2-2	field	359.0	59.8	197.1	182.9	7.1	2.0	14.0	15.61	15.87	0.8*	0.45
Y2-4	indoor	96.1	16.4	52.5	48.7	1.9	3.4	4.2	0.3036	0.3043	0.031**	0.168
Y2-1	indoor	143.6	24.5	78.4	72.7	2.8	5.1	6.3	0.9949	1.0137	0.050**	0.119

*: Composition C−4, **: Pentolite
***: distance between center of the container and ground

of this study was to observe the trajectory of fragments when a steel container exploded, and to clarify their distributions and velocities using both high−speed and flash X−ray photography. In this paper, we focus on fragments flying perpendicular to the direction of the detonation wave propagating inside the container. The velocities and distributions of the fragments measured using two visualization methods are reported.

2. Experiments

2.1 Field explosion tests

Figure 1 is a schematic drawing of the S45C carbon steel container used in this experiment. The length to inner diameter ratio (L/I.D.) of the container was set to be about two and one side of the container was closed. The container was constructed to model a one−ton bomb, and contained TNT as the main explosive. The TNT mass and casing thickness of the container were varied from 0.3 to 16 kg and from 2.7 to 7.1 mm, respectively. The containers used in the tests had similar shapes. The TNT mass to total container mass ratio was set to 0.5. Composition C−4 explosive with L/D=1 was used as a booster and was set in place at the open end of the container. The container was placed transversely on a wooden trestle. The TNT in the container was ignited by a Composition C−4 booster, a dual−detonating fuse and two exploding bridge−wire (EBW) detonators. We used a dual−detonating fuse and two EBW detonators to ensure the initiation of the Composition C−4 booster. The specifications of the containers are summarized in Table 1.

Figure 2 shows a schematic layout of the high−speed photography setup for the field explosion tests. A high−speed camera (Memrecam fx K4, NAC Image Technology, Inc.) with a turning mirror was used to observe the fragments flying in a direction perpendicular to the container. A white cloth, 15.20 m wide and 3.92 m high, (TarpoCanvas #440, Hiraoka & Co., Ltd.) was used as a background screen, or witness sheet, to make it possible to observe the fragments clearly. The distance between the center of the container and the foot of the perpendicular line projected on the witness sheet was 8.52 m. The high−speed camera was placed about 80 m from the point of the explosion. The camera was housed in a wooden box to protect it from damage by flying fragments. The firing system (FS−43, Reynolds Industries Systems Inc.) and measurement apparatus were triggered by a digital delay−pulse generator (BNC555, Berkeley Nucleonics Corporation).

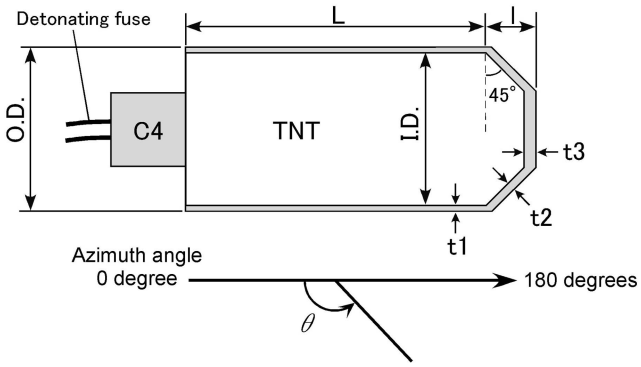

Fig. 1 Schematic diagram of steel container.

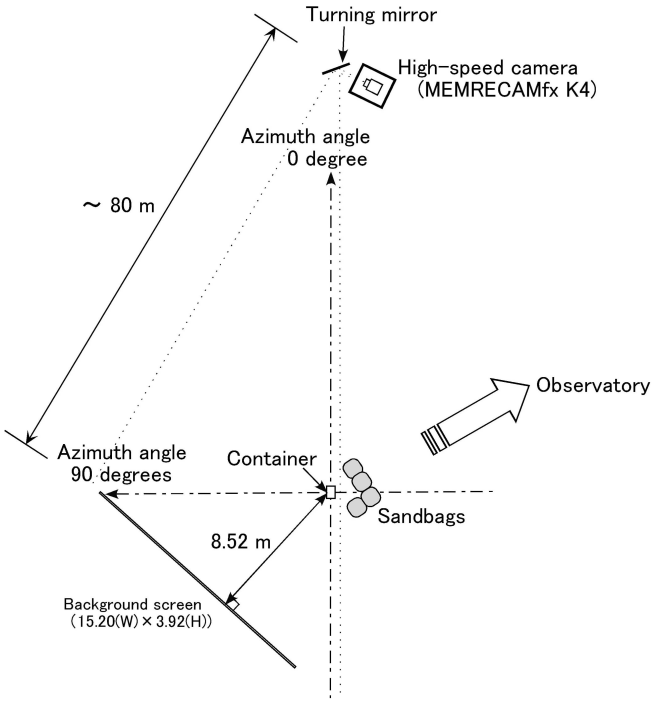

Fig. 2 Schematic layout of high−speed photography setup used in field explosions tests.

2.2 Indoor explosion tests

Flash X−ray photography was used to measure the initial velocity of the fragments in tests conducted at the explosion test facility of Chugoku Kayaku Co., Ltd. The X−ray shadowgraph technique was used to visualize the fragments within the gas cloud produced by the explosion. Images of the flight of the fragments were taken at different

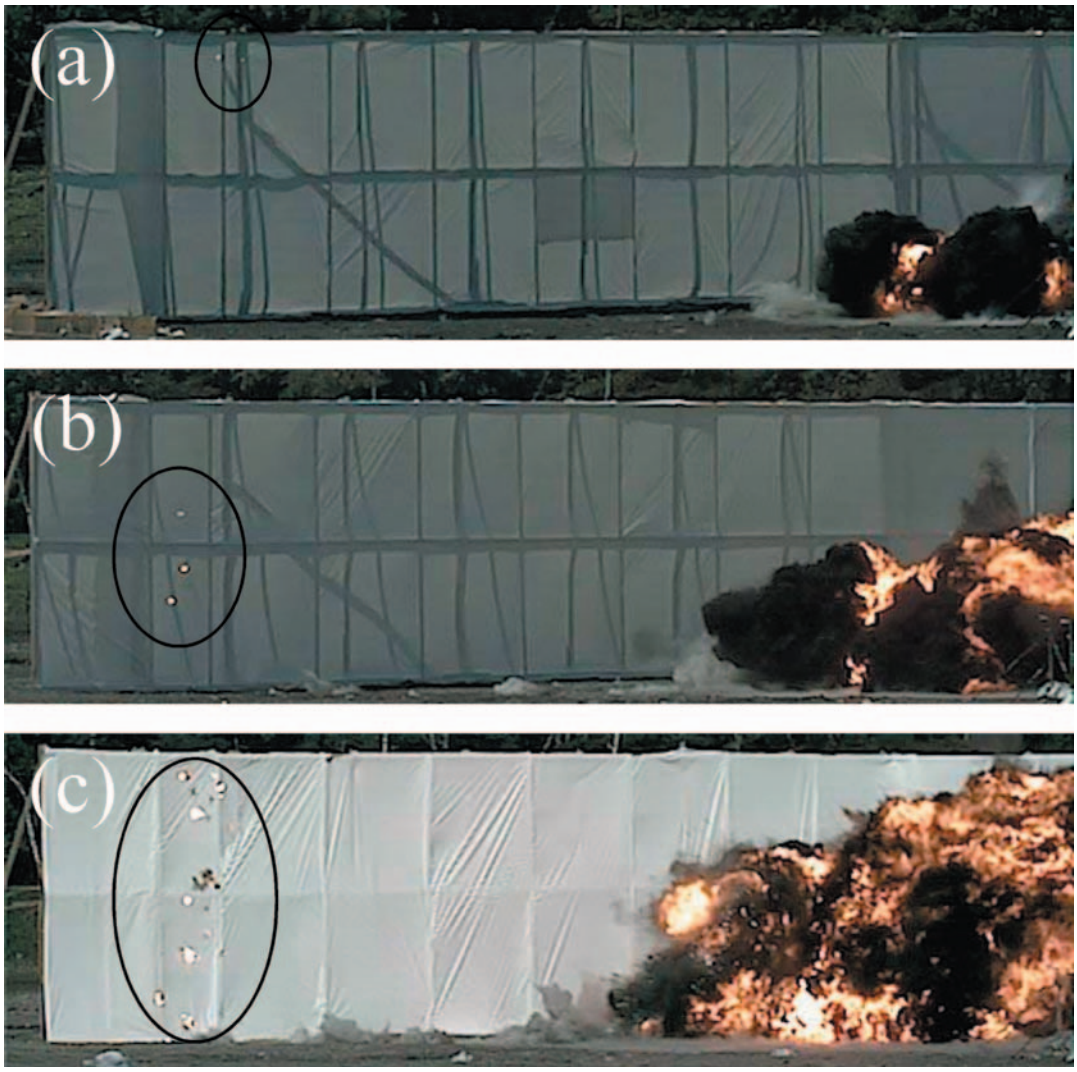

Fig. 3 Typical high−speed photography results.
(a) No. 2−3 at 7.2 ms, (b) No. 2−1−3 at 8.4 ms, (c) No. 2−2 at 6.6 ms after initiation. Notable emissions caused by the impact of fragments on the witness screen are circled.

times using two flash X−ray tubes (model 450, Scandiflash AB). The pulse width of the flash X−ray was 20 ns. The flash X−ray tube was placed 408 and 870 mm from the surface of the container. The flight distance was estimated by accounting for the magnification of the X−ray photographs. The two nails that can be seen in the upper left of the X−ray images in Fig. 7 were used as fiducial marks.

The specifications of the steel containers and explosives used in the indoor explosion tests were almost the same as those used in the field explosion tests, except for the mass of the main charge and booster (pentolite). The containers were filled with 0.3 and 1 kg of TNT. The specifications of the containers used in the indoor explosion tests are summarized in Table 1.

3. Results and discussion

3.1 Field explosion tests

Figures 3 (a)−(c) show typical high−speed photographs taken at 5000 frames per second for different steel containers. Each photograph was taken at the moment an emission was observed on the witness sheet.

The positions of the emissions observed on the witness sheet correspond well with those of the holes made in the witness sheet recovered after the explosion test. These holes were made by flying fragments. Therefore, it is reasonable to suppose that the time at which the emission was observed corresponded to the time at which the fragments impacted the witness screen. This emission can be considered to originate from the plasma generated by the compression of air between a fragment and the witness screen. It was also shown that the number of fragments tends to depend on the thickness of the container casing and the explosive mass. The fastest arrival time for a container fragment to impact the witness screen was 5.8 ms for 16 kg of TNT, 7.6 ms for 4 kg of TNT, and 7.2 ms for 1 kg of TNT. Here, time zero (t_d=0) was defined to be the time at which the EBW detonators were initiated. Arrival time includes the propagation time of the detonating fuse, which is not negligible.

Figure 4 shows a distribution map of the fragments on the witness screen.

Observed fragments were distributed nonuniformly along a horizontal axis. Many fragments were concentrated at around 7.4 m in the horizontal direction on the witness screen. The horizontal distance between the initial position of the container and the position where many

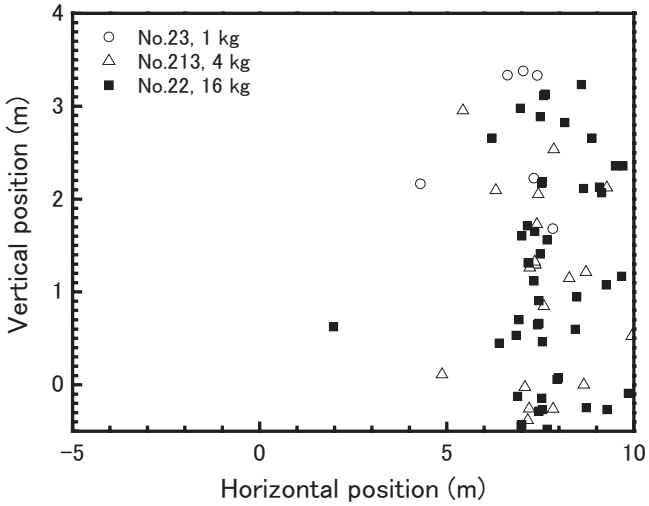

Fig. 4 Distribution map of fragments on the witness screen. ○ : No. 2–3 (TNT 1 kg), △ : No. 2–1–3 (TNT 4 kg), ■ : No. 2–2 (TNT 16 kg). Zero in the vertical direction denotes the center of the container.

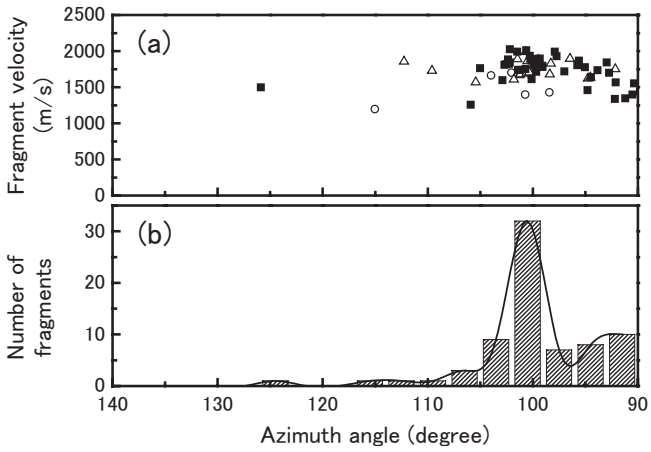

Fig. 5 Azimuth angular distributions of fragment velocity (a) and number of fragments (b). The number of fragments was counted at three–degree intervals. ○ : No. 2–3 (TNT 1 kg), △ : No. 2–1–3 (TNT 4 kg), ■ : No. 2–2 (TNT 16 kg).

fragments were concentrated on the witness screen was about 11.3 m. The azimuthal angle where many fragments concentrated was 100.6 degrees, as described below. On the other hand, the vertical distribution of fragments was uniform. Taken together, these findings reflect the cylindrical shape of the container. The number of fragments increased with an increase in the mass of TNT. The average fragment velocity for all identified fragments is plotted in Fig. 5(a) as a function of the azimuthal angle.

The average fragment velocity was estimated by the time–of–flight (TOF) method, taking the propagation time of the detonating fuse into account. An azimuthal angle of zero degrees is defined as the direction from the center of the container to its open end. Figures 5(a) and (b) show that the velocity and azimuthal angle of the fragments are mainly distributed from 1500 to 2200 $m \cdot s^{-1}$ and from 105 to 90 degrees, respectively. There is a noticeable tendency for many of the fragments to be distributed around an azimuthal angle of 100 degrees. No apparent differences could be found in the fragment distribution of the three

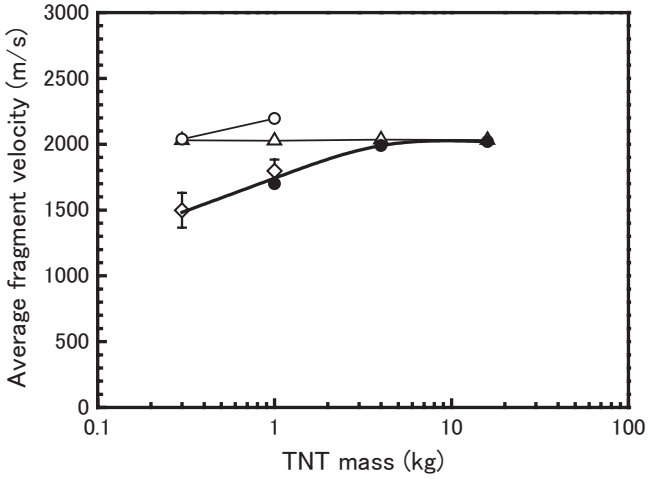

Fig. 6 Fastest fragment velocity measured by TOF method versus TNT mass. ● : high–speed photography, ○ : flash X–ray photography, ◇ : fragment velocity estimated using flash X–ray images under a simple assumption (Error bar of the estimated average velocity was attributed to the mass distribution of fragments (M_f = 0.4~2 g). The thick line is a visual guide.) △ : Gurney velocity (~2030 $m \cdot s^{-1}$).

containers (1, 4, 16 kg). The azimuthal angle at which the fragments concentrate agrees well with that reported in the literature[8].

The velocity of the fastest fragment is plotted against TNT mass (filled circles in Fig. 6). This result indicates that the velocity of the fastest fragment increased and approaches the Gurney velocity[9),10)] (open triangles in Fig. 6) with an increase in the mass of TNT.

3.2 Indoor explosion tests

Figure 7 shows typical flash X–ray photography results. These photographs were taken at (a) 210.1 μs and (b) 436.3 μs after the initiation of the Composition C–4 booster.

This figure shows that the container was broken into many fragments of irregular stick–like shapes. The group of fragments moved to the bottom right of the obtained images, because the explosion in the container was initiated from top to bottom. The fragment velocity was estimated by dividing the flight distance by the time difference between two flash X–ray images. The fastest fragment velocity measured at a distance of around 0.7 m was 2194 $m \cdot s^{-1}$ for 1 kg of TNT, and 2038 $m \cdot s^{-1}$ for 0.3 kg of TNT (Fig. 6).

3.3 Comparison of fragment velocity

Fragment velocity estimated using the Gurney formula[9),10)] was almost constant as indicated by the open triangles in Fig. 6. The Gurney velocities were around 2030 $m \cdot s^{-1}$ for all the containers used in this study, because their container–to–explosive mass ratios were almost the same. However, the fastest measured fragment velocity increased with an increase in TNT mass, as shown in Fig. 6. Furthermore, the fastest fragment velocities observed by high–speed photography (field explosion tests) and by flash X–ray photography (indoor explosion tests) did not agree. The velocity observed with flash X–ray photogra-

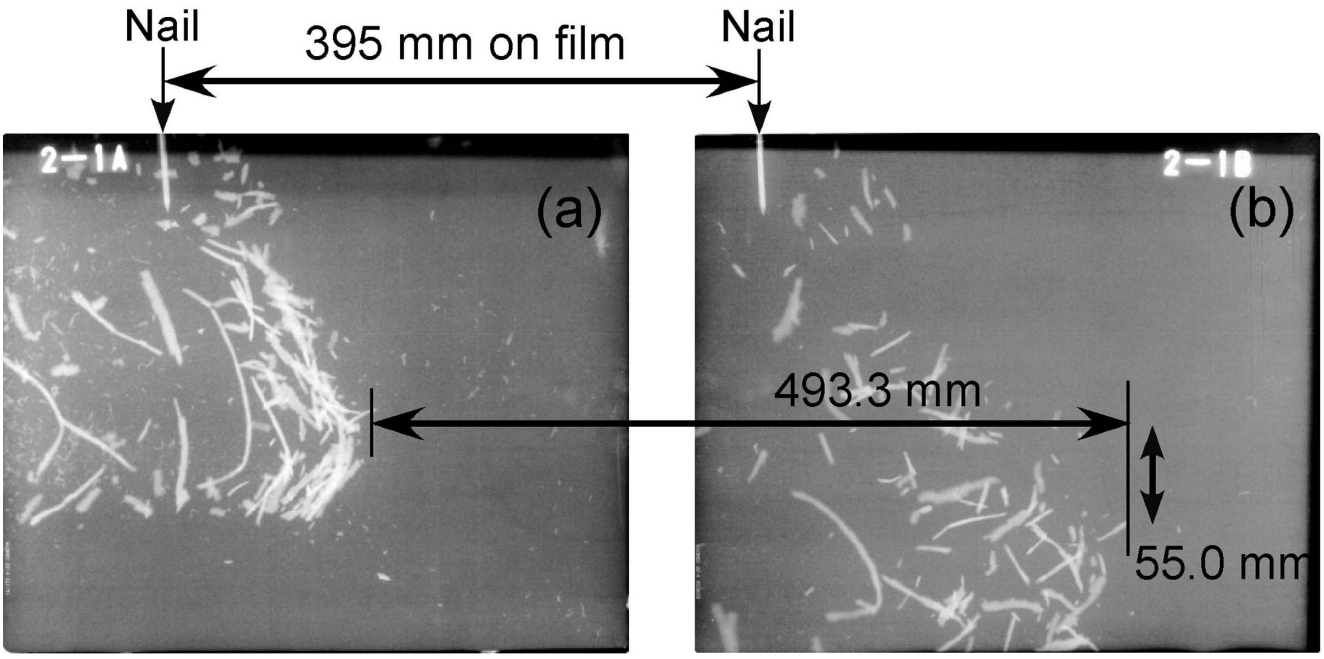

Fig. 7 Typical result of flash X−ray photography (Experiment No. Y2−1).
(a) : 210.1 μs, (b) : 436.3 μs after initiation of Composition C−4 booster. The distance between two nails is 395 mm on film. The flight distances of fragments (493.3 and 55.0 mm) shown in the images were corrected for magnification of images.

phy was higher than that observed with high−speed photography. This difference is clearly apparent in the results obtained for a container with 1 kg of TNT. This difference could have originated from the velocities of fragments hurled outward from the container being reduced by air resistance. Therefore, the velocity measured using the TOF method was lower than that measured using flash X−ray photography. It is important to evaluate the effect of air resistance on fragments, because air resistance is an essential parameter that affects the trajectory of fragments. In this paper, the effects of air resistance on fragment velocity were estimated by the procedures outlined below.

Generally, an object moving through a fluid experiences the forces of both viscosity resistance and inertial resistance. The magnitude of each resistance force depends on the velocity of the object moving in the fluid. In particular, an object moving through a fluid at a relatively high velocity mainly experiences inertial resistance force. The fragment velocity measured in the experiments we conducted exceeded the velocity of sound in air ; therefore, it is reasonable to assume that the dominant resistant force applied to the fragment was inertial resistance. Based on the assumption of Newton's law of inertial resistance, the equation of motion for a fragment is expressed by Eq. (1).

$$M_f \cdot \frac{dV_{(R)}}{dt} = -\frac{C_{d(V)} \cdot rho \cdot A_f \cdot V_{(R)}{}^2}{2} \tag{1}$$

where M_f [kg] is the mass of the fragment under consideration, R [m] is the distance from the reference position, $V_{(R)}$ [m・s^{-1}] is the fragment velocity at a distance R, V_0 [m・s^{-1}] is the initial fragment velocity, $C_{d(V)}$ is the coefficient of inertial resistance, rho [=1.2 kg・m^{-3}] is the density of air, and A_f [m^2] is the projected area of the fragment. A fragment moving in air experiences air resistance in the opposite direction to its motion.

Fragment velocity as a function of distance can be obtained from Eq. (2)[11] by solving Eq. (1) with an initial condition of t=0, R=0, and $V_{(0)}$=V_0, where t [s] is time.

$$V_{(R)} = V_0 \cdot \exp\left[-\left(\frac{C_{d(V)} \cdot rho \cdot A_f}{2M_f}\right) \cdot R\right] \tag{2}$$

The shapes of the fragments generated in a container explosion are irregular, and no two fragments have exactly the same shape. The properties of the fragments, including mass, shape, and projected area, have been investigated for various kinds of shells and bombs[8), 11), 12)]. The relation between the mass (M_f) and projected area (A_f) of a fragment has been reported to be described by Eq. (3)[11] under the assumption that the shapes of the fragments are geometrically similar :

$$M_f = k \cdot A_f^{3/2}, \tag{3}$$

where k [g・cm^{-3}] is the shape factor. The shape factor (k), which has been determined empirically by ballistic tests for many kinds of ammunitions, has been reported in the literature[11]. For example, the shape factor (k) for a fragmentation bomb is 2.61. The shapes of the containers used in the current experiments were considered to be similar to that of a fragmentation bomb. Therefore, we used a shape factor (k) of 2.61 for the containers used in the experiments.

After the field explosion tests, 196 fragments were recovered and their masses ranged from 0.4 to 7.6 g for a 1 kg container (No. 2−3). There were a few fragments with masses of several grams, while most fragments had masses less than 2 grams. The total mass of the recovered fragments was 275.6 g, which is equal to 28.4 % of the initial container mass. The arithmetic average mass of the fragments was 1.41 g. The cumulative number of fragments recovered after an explosion test with a 1 kg container (No. 2−3) is shown by the bar graph in Fig. 8. Here, the cumulative number of fragments means the integrated number of fragments with a mass larger than the

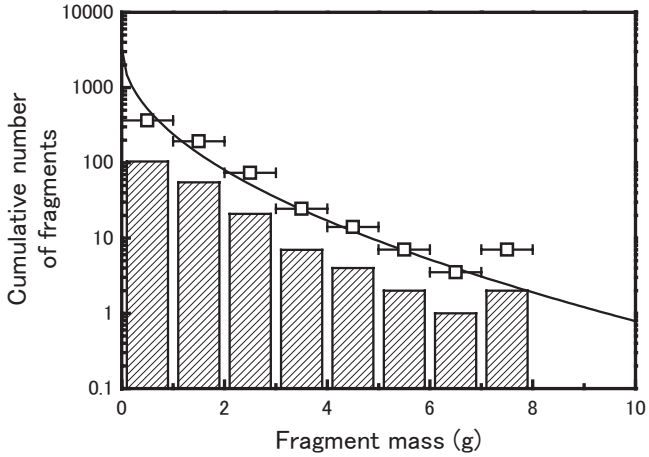

Fig. 8 Comparison of experimental and theoretical cumulative numbers of fragments.
Bar graph : recovered fragments (No. 2–3), □ : estimation using the mass ratio of the initial container and recovered fragments. The solid line indicates the theoretical cumulative number of fragments based on the Mott distribution.

considered fragment mass.

The theoretical cumulative number of fragments for the current container can be estimated by using the formulas reported by Mott[8), 11), 13)]. The cumulative distribution of the fragments (N_f) and the fragment distribution factor (M_A) have been represented by the following equations[11)].

$$N_f = \left(\frac{M_t}{2 \cdot M_A^2}\right) \cdot \exp\left[-\frac{\sqrt{M_f}}{M_A}\right] \tag{4}$$

$$M_A = B_x \cdot t_C^{5/6} \cdot d_i^{1/3}\left(1+\frac{t_c}{d_i}\right) \tag{5}$$

where M_t is the total fragment mass [kg], M_A is the fragment distribution factor [$kg^{1/2}$], M_f is the mass of the fragment under consideration [kg], N_f is the cumulative distribution of the number of fragments with a mass greater than M_f, B_x is the explosive constant (= 3.815 for TNT) [$kg^{1/2} \cdot m^{-7/6}$], t_c is the casing thickness [m], and d_i is the inner casing diameter [m].

The experimental cumulative number of fragments did not agree with the theoretical value, because the theoretical result represents an estimation in which all fragments are recovered. Here, we estimated the ideal cumulative number of fragments by using the mass ratio of the initial container and recovered fragments, under the assumption that all the fragments of the container were recovered in their entirety. The estimated cumulative number of fragments is plotted in Fig. 8. The ideal cumulative number estimated by recovered fragments agreed well with that of the theoretical estimation. This result indicates that the fragments distribute exactly in accordance with the Mott distribution. It was also shown that the distribution of the recovered fragments did not include artifacts due to manual recovery, although the recovered fragments only accounted for part of the total mass of the container. Therefore, it would be reasonable to assume that the distribution of the fragments that reached the witness screen was almost the same as that of the recovered fragments.

The coefficient of air resistance ($C_{d(V)}$) includes all complex dependencies and is usually determined experimentally[11), 12)]. The $C_{d(V)}$ value for irregular fragments generated by the explosion of bombs and ammunitions has been reported in the literature[11)]. Eleven data points for the value of $C_{d(V)}$ for velocities ranging from 0 to 3060 $m \cdot s^{-1}$ have been given in tabular form[11)]. In order to obtain the interpolated value of $C_{d(V)}$ at any velocity, we constructed a natural cubic spline with 10 piecewise cubic polynomials between the 11 data points. The position of the knots was defined as being the same as that of the given 11 data points. The obtained parameters of the 10 cubic polynomials are listed in Table 2.

By substituting Eq. (3), the $C_{d(V)}$ value and the velocity measured by flash X−ray photography into Eq. (1), we estimated the trajectory of fragments with masses from 0.4 to 2.0 g using the difference calculation with intervals of ΔR =0.1 m. The average fragment velocity from the container to the position where many fragments concentrated on the witness screen was 1684 $m \cdot s^{-1}$ for a 0.4 g fragment, and 1886 $m \cdot s^{-1}$ for a 2 g fragment.

For a container with 0.3 kg TNT, the fragment velocity was estimated using the same procedure because the distribution of the fragments is scale invariant, as indicated by the Mott distribution. The estimated average velocity of fragments is also shown by an open rhombus in Fig. 6. The error bar of the estimated average velocity was attributed to the mass distribution of fragments (M_f = 0.4~2

Table 2 Obtained parameter of ten cubic polynomials.
A cubic polynomial is defined as : $C_{d(V)} = a \cdot (V - V_{from})^3 + b \cdot (V - V_{from})^2 + c \cdot (V - V_{from}) + d$. V varies from V_{from} to V_{to}.

Function number	Velocity range ($m \cdot s^{-1}$)		Parameter			
	from (V_{from})	to (V_{to})	a	b	c	d
1	0	204	2.73E−09	0.00E+00	−1.14E−04	1.08
2	204	272	5.35E−08	1.67E−06	2.27E−04	1.08
3	272	340	−6.21E−08	1.26E−05	1.20E−03	1.12
4	340	408	−5.94E−08	−9.39E−08	2.05E−03	1.24
5	408	476	4.52E−08	−1.22E−05	1.21E−03	1.36
6	476	544	5.81E−09	−2.99E−06	1.76E−04	1.40
7	544	680	5.42E−09	−1.80E−06	−1.49E−04	1.40
8	680	1020	−3.06E−10	4.08E−07	−3.39E−04	1.36
9	1020	1700	−3.36E−11	9.58E−08	−1.67E−04	1.28
10	1700	3060	−6.69E−12	2.73E−08	−8.36E−05	1.20

g). As shown in Fig. 6, the average fragment velocity estimated by a simple assumption agreed reasonably well with that measured by the TOF method. We have confirmed that the discrepancy between the fragment velocities measured in the field and the indoor explosion tests can be explained by using a simple formula for the current experimental conditions. It was shown that this method is useful for estimating the velocity history of fragments flying through the air. It is expected that the estimated velocity can be used as fundamental information for the development of safe measuring techniques for reducing the effects of explosions and damage caused by fragment impact.

4. Conclusion

Explosion tests were performed on steel containers filled with TNT to measure fragment velocity, angle, and distribution. Images of flying fragments were recorded using both high−speed and flash X−ray photography. Many fragments were distributed at azimuthal angles of about 100 degrees. The fragment velocities measured using the two methods did not agree. This discrepancy between the measured fragment velocities could be satisfactorily explained by assuming that the fragment velocity depends solely on air resistance.

References

1) "1996 Protocol to the Convention on the Prevention of Marine Pollution by Dumping of Wastes and Other Matter, 1972 and Resolutions Adopted by the Special Meeting", http : //www.env.go.jp/council/toshin/t063−h1506/ref_01.pdf
2) W. E. Baker, *"Explosions in Air"*, Univ. of Texas Press (1973).
3) M. M. Swisdak Jr., NSWC Technical Report, Explosion Effect and Properties, Part1−Explosions in Air, Naval Surface Weapons Center, (1975).
4) R. W. Prugh, Process Safety Progress, **18**, 5 (1999).
5) P. C. Chou, J. Carleone, W. J. Flis, R. D. Ciccarelli and E. Hirsch, Propellants, Explosives, Pyrotechnics, **8**, 175 (1983).
6) E. Hirsch, Propellants, Explosives, Pyrotechnics, **11**, 6 (1986).
7) F. P. Lees, "*Loss Prevention in the Process Industries 2nd. ed.*", vol. 2, 17 Explosion, p. 229 (1996), Butterworth−Heinemann.
8) AMC Pamphlet 706−245, "Ammunition Series Section2, Design for Terminal Effects", Headquarters, U.S. Army Material Command, July (1964).
9) A. C. Victor, Propellants, Explosives, Pyrotechnics, **21**, 90 (1996).
10) B. T. Fedoroff and O. E. Sheffield, Encyclopedia of Explosives and Related Items, vol. 6, G195 (1974).
11) "Manual on NATO safety principles for the storage of ammunition and explosives AASTP−1 Edition1", NATO Group of Experts on the Safety Aspects for Transportation and Storage of Military Ammunition and Explosives, (2006).
12) F. McCleskey, "Drag Coefficients for Irregular fragments", Naval Surface Weapon Center, NSWC−TR−87−89 (1988).
13) D. Grady, "*Fragmentation of Rings and Shells*", Springer press (2006).

高速度及びフラッシュX線撮影法を用いた爆発実験における金属製容器の破片速度測定

若林邦彦†，保前友高，石川弘毅，黒田英司，松村知治，中山良男

爆薬を充填した金属製容器の爆発実験を実施し，爆発時に発生する飛散物の速度や方向，分布等に関する基礎的なデータを取得した。金属製容器にTNT爆薬を充填し，１トン爆弾を模擬した数種類の試験体を使用した。容器の長さと内径の比（長さ／内径）は約２である。爆発によって発生した飛散物を撮影するために，野外実験では高速度カメラ，室内実験ではフラッシュX線装置を使用した。試験体容器の中心から容器開放端方向を方位角０度と定義した場合，多くの破片は方位角100度付近に分布していることが示された。TNT爆薬量１kgの容器爆発の場合，野外実験では，爆点から11.56 ± 0.01m離れた位置においてタイムオブフライト法によって測定された最速の飛散物速度は1700± 50 m・s^{-1}であった。しかしながら，室内実験においてフラッシュX線撮影で測定した飛散物の初速度は2194m・s^{-1}であり，野外実験の結果と一致しなかった。飛散物速度が空気抵抗のみに依存すると仮定すると，測定された飛散物速度の不一致が良く説明できることが分かった。

独立行政法人産業技術総合研究所安全科学研究部門爆発安全研究コア
〒305−8565　茨城県つくば市東1−1−1中央第五　Tel : 029−861−4792, Fax : 029−861−4783
†Corresponding address : k−wakabayashi@aist.go.jp